

pubs.acs.org/JPCB Article

Development of AMOEBA Polarizable Force Field for Rare-Earth La³⁺ Interaction with Bioinspired Ligands

Elizabeth E. Wait, Justin Gourary, Chengwen Liu, Erik D. Spoerke, Susan B. Rempe,* and Pengyu Ren*



Cite This: J. Phys. Chem. B 2023, 127, 1367-1375



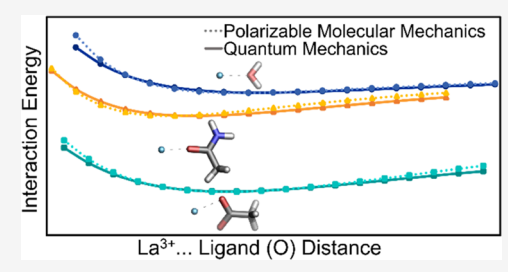
ACCESS I

III Metrics & More

Article Recommendations

Supporting Information

ABSTRACT: Rare-earth metals (REMs) are crucial for many important industries, such as power generation and storage, in addition to cancer treatment and medical imaging. One promising new REM refinement approach involves mimicking the highly selective and efficient binding of REMs observed in relatively recently discovered proteins. However, realizing any such bioinspired approach requires an understanding of the biological recognition mechanisms. Here, we developed a new classical polarizable force field based on the AMOEBA framework for modeling a lanthanum ion (La³⁺) interacting with water, acetate, and acetamide, which have been found to coordinate the ion in proteins. The parameters were derived by comparing to high-level *ab initio* quantum mechanical



(QM) calculations that include relativistic effects. The AMOEBA model, with advanced atomic multipoles and electronic polarization, is successful in capturing both the QM distance-dependent La³⁺-ligand interaction energies and experimental hydration free energy. A new scheme for pairwise polarization damping (POLPAIR) was developed to describe the polarization energy in La³⁺ interactions with both charged and neutral ligands. Simulations of La³⁺ in water showed water coordination numbers and ion-water distances consistent with previous experimental and theoretical findings. Water residence time analysis revealed both fast and slow kinetics in water exchange around the ion. This new model will allow investigation of fully solvated lanthanum ion-protein systems using GPU-accelerated dynamics simulations to gain insights on binding selectivity, which may be applied to the design of synthetic analogues.

INTRODUCTION

Rare-earth metals (REMs), comprising lanthanides plus scandium and yttrium, are essential to many modern industries, including usage in electronics, car batteries, wind turbines, military equipment, medical imaging, and cancer therapies. 1,2 The extraction and refinement of REMs has declined precipitously in the United States due to the difficult, expensive, labor-intensive, hazardous, and environmentally detrimental mining and separation methods currently used for high-volume REM processing. 1,2 REMs are often dilute or come in complex mixtures, making target REMs difficult to harvest and separate, particularly from other chemically similar lanthanides. Traditional refining methods employ synthetic chelators, which are not highly specific and thus require high-quality primary sources that contain few competing metal ions. Even so, several chromatographic separation steps are typically required. Development of a new technique that could not only enable efficient, environmentally friendly harvesting from conventional sources but could also take advantage of lower-grade sources (such as electronic waste, coal ash, and acid mine drainage) would be highly attractive and increase global availability of these critical resources. 1-3 Here, we seek to develop advanced molecular simulation tools to enable a more accurate understanding of fundamental interactions between the rare-earth

lanthanum and ligands inspired by biological systems recently observed to bind REMs with remarkable effectiveness.

Previously, REMs were thought to be nonessential in biology, even if some organisms were able to bind them. Protein—REM binding studies were done by replacing the s- and d-block metals in metal-binding proteins with REMs. The proteins could often still accommodate the larger REM ions but did not bind the REMs specifically. Instead, proteins would take up the other ions in solution, such as calcium. In 2011, it was discovered that some methylotrophic bacteria use REM ions in pyrroloquinoline quinone (PQQ)-dependent alcohol dehydrogenases (ADHs). In 2014, a thermoacidophilic methanotroph (*Methylacidiphilum fumariolicum SolV*), which requires REMs to survive, was found in a volcanic mudpot by Pol et al. In 2018, an enzyme from the methylotrophic bacteria *Methylobacterium extorquens* was found to bind lanthanum ions (La³+) selectively at four EF-hand metal coordination sites and subsequently named lanmodulin. By

Received: October 14, 2022 Revised: January 18, 2023 Published: February 3, 2023





taking inspiration from biological extremophiles that depend on highly selective binding of lanthanide-group REMs from dilute, natural, or mixed sources, it may be possible to design compounds to filter out REMs from waste streams. 1,2,5 Knowledge of the mechanism of lanmodulin—REM binding is essential to understanding its desirable selectivity function.

The REM ions are found to interact primarily with carboxyl groups in highly electrostatic interactions. REM ions are large, especially the early lanthanides, and consequently have a high coordination number (CN 8-9). In interactions with lanmodulin, the early lanthanides (La-Nd) bind with similar affinities (K_d^{apparent} 5-25 pM at pH = 7.2 at the three highaffinity sites, and $K_a^{\text{apparent}} \gg 1 \, \mu\text{M}$ at pH = 6 at the weak site), forming contacts with eight oxygens of five carboxylate groups from side chains and one backbone carbonyl in lanmodulin. Binding is cooperative and involves a large conformational change. Although part of the specificity may involve hydrogen bonding of a proline to its neighboring residue, the large conformational change could allow for further specificity. ^{1,2} The binding is also reversible as lanmodulin releases REM ions at low pH, similar to synthetic chelators. While lanmodulin does retain its fast kinetics, quantitative yields, and high selectivity for REMs over competing ions at low pH and fairly high pH industrial conditions, further engineering is still necessary because lanmodulin does not differentiate much between elements in the lanthanide series ranging from La to Nd, and immobilization would be beneficial for large-scale industrial applications beyond laboratory conditions.

Molecular dynamics simulations can provide thermodynamic and mechanistic insights with atomic-level details beyond the reach of experimental measurement. It is extremely challenging to develop general and balanced fixed-charged force fields for monovalent or higher-valence ions that can be applied to study ion interactions with a wide range of chemical groups, as fixedcharge force fields do not account for electrostatic many-body polarization. 6-14 Special treatments were devised to enable the simulation of high-valence ions with fixed-charge water models 15,16 and reduced models of proteins. 17-21 These simulations were short and limited to small system sizes, but hydration properties could still be assessed with reasonable accuracy upon parameter optimization. However, simulating ion binding and unbinding to protein and other biomacromolecules remains a significant challenge, motivating further development of polarizable force fields. The AMOEBA (atomic multipole optimized energetic for biomolecular applications) force field is polarizable, using a more advanced electrostatic model than Amber and CHARMM fixed-charge force fields. ^{22–26} AMOEBA was recently successful in describing the mechanism of potassium ion conduction through channel proteins, which are difficult systems to simulate due to the importance of complex electrostatic interactions. 10 Amber and CHARMM polarizable force fields are actively under development, but no study for trivalent ions has been reported.^{27–30}

A study of La³⁺ and Eu³⁺ ions based on the AMOEBA model was reported in 2005. This early study was the first application of polarizable force fields to lanthanides in water. The QM calculations used for parameterization did not account for relativistic effects of water binding energy. Short dynamic simulations were performed to investigate ions in water without calculating hydration free energy for which the experimental data are available.³¹ In addition, ion interaction with other chemical groups such as amide or acetate was not examined. Vázquez-Montelongo et al. developed parameters for the

AMOEBA simulation of $\mathrm{Gd^{3+}}$, $\mathrm{Dy^{3+}}$, and $\mathrm{Ho^{3+}}$ using ion—water interaction energies obtained at the MP2/SDD/6-311G(d,p) theory level, in addition to previously reported QM EDA data. The ions were then simulated in water, EMIm, and $\mathrm{EtSO_4}$ using AMOEBA to investigate water-exchange dynamics. There was good agreement with experimental data for the thermodynamic properties, and the experimental trends for exchange rate coefficients were reproduced.

Recently, parameters for divalent ions among the lanthanide series (Sm²⁺ and Eu²⁺) were obtained for simulations with AMOEBA force-field models.¹¹ Binding energies were calculated at various distances using electronic structure calculations based on ab initio quantum mechanics (QM) at the DLPNO-CCSD(T) theory level and subsequently compared with the AMOEBA model. Radial distribution functions of water around Sm²⁺ and Eu²⁺ in bulk solution and water-exchange times were obtained from molecular dynamics simulations, revealing a coordination number between 8 and 9. No hydration thermodynamics were reported. Furthermore, lanthanides typically carry +III charge in solution. A 2012 study by Marjolin et al. involved creation and validation of a SIBFA (sum of interaction between fragments ab initio computed) model for the thorium (+IV) cation, with transfer to lanthanum (+III) and lutetium (+III) and subsequent comparison to QM data. The SIBFA model was more complex than AMOEBA, and it was in excellent agreement with ab initio methods for distancedependent interaction energies. The SIBFA force field for biomolecules and its supporting simulation platform are still under development. Therefore, a new AMOEBA model for La³⁺ is needed for large-scale molecular dynamics simulations of ion binding with proteins and synthetic materials.

This work focuses on the development of a high-quality and comprehensive La³⁺ model for the simulation of ion interaction with biomolecular fragments using the polarizable AMOEBA force field. Polarizable potentials are well suited to capture many-body electrostatic effects in a manner transferable among different chemical and physical environments. AMOEBA parameters for La³⁺ were obtained by comparing to QM and experimental bulk data. We found that the effects of polarization are strong between the ion and acetate, and it was necessary to develop a new pairwise scheme to address polarization damping. Overall, the parameters for the AMOEBA polarizable model were reasonably transferable from the gas to liquid phase environments. This work will enable us to perform accurate molecular dynamics simulations of La³⁺ binding to proteins such as lanmodulins in the future. ^{1,2,5,36}

METHODS

The AMOEBA polarizable force field was used to study the interactions between La^{3+} and three ligand compounds, namely, water (H_2O) , acetate (CH_3COO^-) , and acetamide (CH_3CONH_2) . These compounds were chosen for parameterizing La^{3+} interactions as they were found to be responsible for most of the important interactions of La^{3+} in protein binding pockets on the Protein Data Bank. Therefore, these interactions are the most important for us to describe. A full description of the AMOEBA functional forms can be found in our previous publications. 38,39

In our model, La³⁺ interacts with the ligand compounds via permanent electrostatics, polarization, and van der Waals interactions. The atomic charge on the ion is set to 3.0 without

permanent dipoles and quadrupoles. Polarizability is accounted for via an atomic dipole induction scheme

$$\mu_i^{\text{ind}} = \alpha_i \left(\sum_j T_{ij} M_j + \sum_j T_{ij}^{11} \mu_j^{\text{ind}} \right)$$
(1)

where the first term on the right-hand side represents the contribution from permanent multipoles, and the second represents the induced dipoles. T_{ij} is the interaction matrix between atoms, and M_j are the permanent charge, dipole, and quadrupole moments.

The dipole polarization is damped via Thole's smeared charge distributions to avoid the so-called "polarization catastrophe" at very short distances

$$\rho = \frac{3a}{4\pi} e^{(-au^3)} \tag{2}$$

where $u(r) = r_{ij}/(\alpha_i \alpha_j)^{1/6}$ is the polarizability-scaled distance between atoms i and j, r_{ii} is the real distance, α is the atomic polarizability, and a is the dimensionless damping factor corresponding to the width of the charge distribution.⁴⁰ The atomic polarizability parameter for La³⁺ was derived from highlevel quantum chemistry calculations. In the AMOEBA model, a universal damping factor of 0.39 is used for the organic/ biomolecules and monovalent atomic ions. Multivalent ions in AMOEBA typically require a smaller damping factor to better capture ion-ligand energies calculated from quantum mechanical simulations. When two atoms have different damping factors, the small one takes precedence. This parameterization is straightforward, but it also introduces limitations, especially when the ion binds to multiple different ligands as it does in lanmodulin protein binding pockets. In this case, different damping factors may be needed to describe the interactions better. To overcome this limitation, the Tinker software package⁴¹ has been modified to support a special damping parameter for any pair of atoms, called POLPAIR. Other schemes for polarization damping have been developed previously.42

The AMOEBA force field uses the Halgren's buffered-14-7 potential (eq 3) to describe van der Waals (vdW) interactions

$$E_{\text{vdW}} = \varepsilon_{ij} \left(\frac{1+\delta}{\sigma_{ij} + \gamma} \right)^{7} \left(\frac{1+\gamma}{\sigma_{ij}^{7} + \gamma} - 2 \right)$$
(3)

Here, $\sigma_{ij} = \frac{r_{ij}}{r_{ij}^0}$, with r_{ij} being the separation between the two atoms. Additionally, fixed values of $\delta = 0.07$ and $\gamma = 0.12$ were used. The radius (r_{ij}^0) and well depth (ε_{ij}) between any two atoms are calculated using combining rules from eqs 4 and 5, respectively

$$r_{ij}^{0} = \frac{(r_{ii}^{0})^{3} + (r_{jj}^{0})^{3}}{(r_{ii}^{0})^{2} + (r_{jj}^{0})^{2}}$$
(4)

$$\varepsilon_{ij} = \frac{4\varepsilon_{ii}\varepsilon_{jj}}{(\sqrt{\varepsilon_{ii}} + \sqrt{\varepsilon_{jj}})^2} \tag{5}$$

Similar to the polarization damping described above, pairwise vdW parameters can also be applied to ion and ligand atoms to add extra flexibility. The four La³⁺ parameters described, polarizability (α) , Thole damping factor (a), vdW radius (r_0) , and vdW minimum energy distance (ε) , were developed by

fitting to quantum chemical distance-dependent interaction energy curves in which the ligand was fixed to its equilibrium geometry, as determined by an ion–ligand geometry optimization calculation. In the case of water, experimental hydration free energy data were also used to determine the final parameters. In addition, pairwise polarization damping and van der Waals parameters were developed to describe the interaction of La³⁺ with the acetate and acetamide ligands better. All QM calculations were performed using ORCA Quantum Chemistry Software. ⁴⁵

As relativistic effects may have large impacts on rare-earth metal ion interactions, structures of La³⁺ complexed with a single water, acetate, and acetamide were first optimized at MP2 with the ZORA-DEF2-TZVP relativistic basis set⁴⁶ and Def2-TZVP/C correlation basis set. Distances between the La³⁺ ion and the ligands were varied while keeping the coordinates otherwise fixed to the optimized structure for each monomer. For monodentate ligands (water and acetamide), the ion was moved along an axis defined by the positions of the ion and the closest atom on the ligand. For acetate, a bidentate ligand, the axis was defined by the position of the ion and the average position of the two closest atoms on the ligand. Single point energies were then calculated at the DLPNO-CCSD(T) theory level⁴⁷ with the same basis set and plotted with respect to the change in distance to create interaction energy curves for each pair. A basis set superposition error (BSSE) correction was performed via a procedure similar to that used by Hong et al. (details in SI).48 All QM calculations were performed using ORCA Quantum Chemistry Software. 45

The polarization damping and vdW parameters were optimized against the QM distance-dependent interaction curves for all three ion-ligand pairs using ForceBalance software.⁴⁹ La³⁺ parameters were optimized based on QM interaction energies of ion-water, as well as the experimental hydration free energy for La³⁺ reported by Marcus.⁵⁰ Greater weight was placed on the points nearest to the equilibrium distance to better characterize the La³⁺...CH₃COO⁻ pairwise interactions. This strategy enables user specification of polarization strength parameters for unique atom-type pairs for cases where the default parameter value is inadequate. Finally, energies of each complex at the varied pairwise distances are calculated with Tinker's ANALYZE.x program using the assigned AMOEBA parameters. These results are shown on the interaction energy plots for comparison with the QM data. Structures and parameters for complexes near the minima are included in the Supplemental File "input.txt."

Hydration free energy of an ion is an important thermodynamic property from experiment that characterizes the strength of ion and water interactions.⁵¹ In our study, hydration free energies were calculated using double decoupling with the Bennett Acceptance Ratio (BAR) algorithm. In this method, a La³⁺ ion is "grown" in a periodic box of water by gradually turning on its van der Waals and electrostatic interaction components over the course of 26 NPT simulations using a procedure similar to that described by Wu et al.⁶ A cubic box of \sim 30 Å on a side, containing 894 water molecules was used. The scaling parameters of electrostatics and van der Waals interactions follow the procedure: $(0.00, 0.00) \rightarrow (0.00, 0.45)$ \rightarrow (0.00, 0.52) \rightarrow (0.00, 0.56) \rightarrow (0.00, 0.57) \rightarrow (0.00, 0.60) \rightarrow $(0.00, 0.62) \rightarrow (0.00, 0.64) \rightarrow (0.00, 0.67) \rightarrow (0.00, 0.70) \rightarrow$ $(0.00, 0.75) \rightarrow (0.00, 0.80) \rightarrow (0.00, 0.85) \rightarrow (0.00, 0.90) \rightarrow$ $(0.00, 0.95) \rightarrow (0.00, 1.00) \rightarrow (0.10, 1.00) \rightarrow (0.20, 1.00) \rightarrow$ $(0.30, 1.00) \rightarrow (0.40, 1.00) \rightarrow (0.50, 1.00) \rightarrow (0.60, 1.00) \rightarrow$

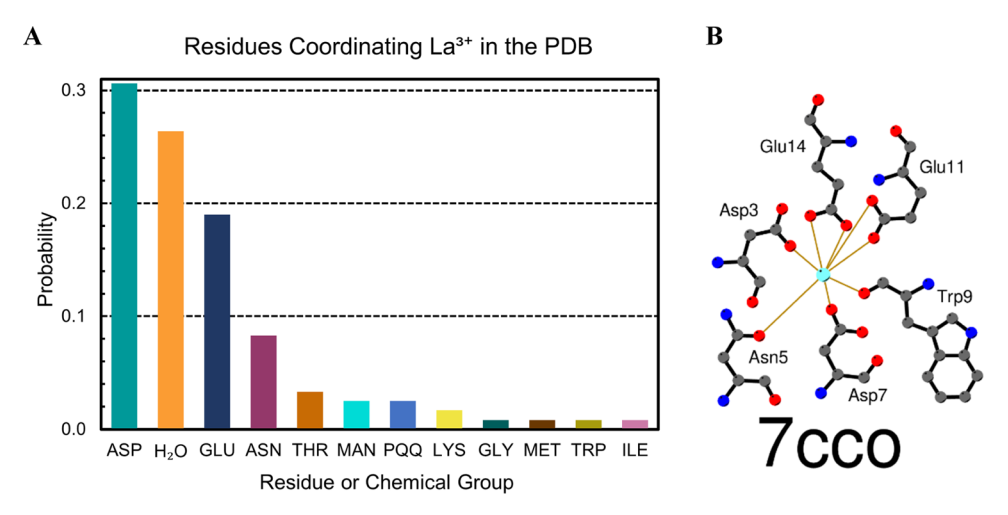


Figure 1. (A) Residues and groups found to coordinate La^{3+} ions directly in PDB entries are largely oxygen-containing. Aspartate and glutamate are the most common residues in the binding pocket, but water is also often present. Note that PQQ is a cofactor that is involved in reactions of alcohol dehydrogenases, which sometimes depend on REMs. (B) Illustration of La^{3+} coordination by oxygens in the lanthanide binding tag (LBT3) (7CCO.pdb). The La^{3+} ion is coordinated by seven oxygens of side-chain carboxylate groups and one from a backbone carbonyl. Figure was made using LigPlot+. S5

 $(0.70, 1.00) \rightarrow (0.80, 1.00) \rightarrow (0.90, 1.00) \rightarrow (1.00, 1.00)$. Long-ranged electrostatic interactions were modeled using particle mesh Ewald summation with a 7 Å cutoff in real space and a 5th order spline in reciprocal space. A 1.25 ns NPT simulation was performed at each lambda value, with a 2 fs time step and a 2 ps save interval and a total production time of 32.5 ns. The last 1.0 ns trajectory at each lambda window was used as production to perform BAR free energy analysis. The temperature was maintained at 300 K with a Bussi thermostat. A Monte Carlo barostat was used to maintain the pressure at 1 atm. All of the MD simulations were performed using Tinker9 software with GPU support. Sample 1.00 in 1.00 i

Finally, to characterize the structural and dynamic properties of La³⁺ in water, the radial distribution function (RDF), coordination numbers, and water residence time (WRT) have been examined from the MD simulations. The RDF of La³⁺oxygen pair was calculated using the Tinker program RADIAL.X. The first solvation shell cutoff in the calculation of the water residence time was 4.0 Å. Any water molecules within this cutoff were considered "resident" molecules. The time they stayed "resident" was counted to calculate the residence time. The coordination numbers were computed by integrating the RDF radially over distance, with the shell volume taken into account. Additional sets of molecular dynamics simulations have been performed using the optimal parameters derived above. Specifically, it is found that WRT can be either long or short. Therefore, we performed simulations for 10 ns and 1.2 ns by saving the trajectories every 4 ps and 0.01 ps, respectively. The simulation settings have been kept the same as above, except for the save intervals and total time length. The WRT was calculated with a Python script in which the LOOS analysis tool⁵⁴ has been employed.

■ RESULTS AND DISCUSSION

We first investigated the composition of binding sites of lanthanum binding proteins collected from the Protein Data Bank (PDB) to understand better which residues are typically involved (see PDB codes in Table S1).³⁷ We found that about 85% of the residues found in the binding sites were water, aspartic acid, glutamic acid, and asparagine (Figure 1A).⁵⁵ The

atoms in close proximity to the ion were exclusively oxygens, largely from acetate and, secondarily, amide functional groups. An example La³⁺ coordination in a binding pocket by oxygens is shown in Figure 1B, with additional examples in Figure S1. It was observed that the acetate groups serve as the primary driver of binding, while the amide groups stabilize the pocket. Accordingly, we selected water, acetate, and acetamide as model compounds to parametrize lanthanum. As described in the Methods section, structures of La³⁺ in complex with each of these three ligands were optimized using QM methods. Equilibrium complex geometries are shown in Figure 2, with La³⁺···CH₃COO⁻ having the shortest interaction distance.

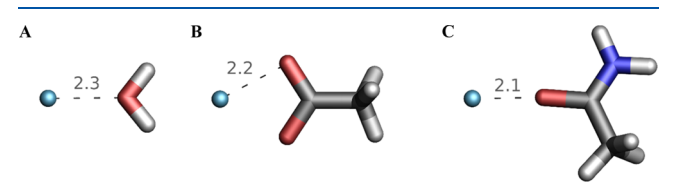


Figure 2. QM-optimized geometries for La^{3+} interactions with (A) water, (B) acetate, and (C) acetamide. Figure was created using Pymol.⁵⁷

By targeting the QM interaction energies and the experimental hydration free energy (in the case of water), parameters for La³⁺ have been optimized and are listed in Table 1. Four parameters have been derived in the case of water, namely, atomic polarizability (α), damping factor (a), vdW radius (R_0), and well depth (ε). The atomic polarizability parameter 1.66 was kept the same in the case of acetate and acetamide. For acetate and acetamide molecules, a new set of atomic polarizabilities⁵⁶ were previously derived, and we called this model AMOEBA22. In addition, we found that a special pair of interactions are necessary to describe the energy curve satisfactorily. This includes the pairwise damping factor and pairwise vdW interaction parameters.

La³⁺...Water Interaction. Ion binding to proteins requires the desolvation of ions from their water environment. Thus, understanding and reproducing the ion (de)solvation free energy is essential. In addition, water molecules may also

Table 1. Damping Factor (a), vdW Radius (R_0), and Well Depth (ε) Parameters for the La³⁺ AMOEBA Model Obtained by Fitting to QM Interaction Energy and Experimental Hydration Free Energy Data¹

	а	R_0 (Å)	ε (kcal/mol)
La ³⁺ ···water	0.250	3.920	0.940
AMOEBA09			
La ³⁺ ···O (acetamide)	0.349	3.300	0.313
La ³⁺ ···C (acetamide)		3.986	0.909
La ³⁺ ···O (acetate)	0.192	3.592	0.259
AMOEBA22			
La ³⁺ ···O (acetamide)	0.299	3.300	0.302
La ³⁺ ···C (acetamide)		3.954	0.829
La ³⁺ ···O (acetate)	0.152	3.632	0.228

¹The value for the damping factor (a) is 0.25, identical to oxygen in water, unless otherwise specified. The atomic polarizability (α) parameter for La³⁺ is 1.660 (Å³). For other polarizability parameters, see Table S2.

participate as ligands in the protein pocket, which is demonstrated by their common presence in the lanthanum binding protein pockets (Figure 1A). To begin characterizing the interaction between La³⁺ and water, QM optimization was used to find a stable geometry for the La³⁺···H₂O complex. Following optimization, we obtained single point energies at varied interaction distances via QM calculation. We then performed single point MM energy calculations using AMOEBA09 with the new parameter values and plotted these results for comparison. Interaction energies were plotted for complexes at intermolecular distances ranging from 1.59 to 3.29 Å (Figure 3). The equilibrium interaction distance was found to

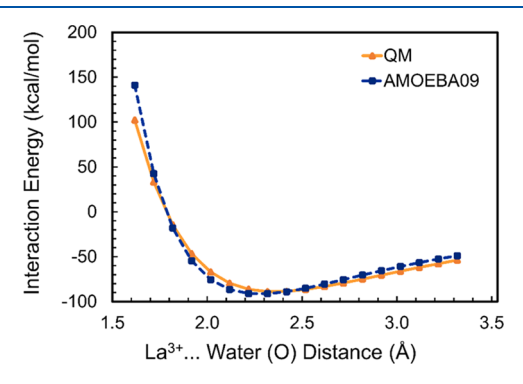


Figure 3. Interaction energies for the La³⁺···H₂O complex from QM and MM (AMOEBA09) calculations.

be 2.3 Å by both QM and AMOEBA09, with energies of -88.9 and -91.27 kcal/mol, respectively. The AMOEBA09 model was able to capture nearly the entire curve with excellent agreement to the QM results, up to the repulsive wall. For comparison, the previously mentioned theoretical work by Marjolin et al. reported an interaction distance of about 2.4 Å at an energetic minimum of ~ -90 kcal/mol using a SIBFA (sum of interaction between fragments *ab initio* computed) polarizable potential at the MP2 theory level, with a slightly lower energy obtained using the MRCI (multireference configuration interaction) method, and -82.6 kcal/mol according to RVS/CSOV (restricted variational space/constrained space orbital variation) energy decomposition at the HF level. ³³

Our hydration free energy calculations display excellent agreement with experiment as well. The calculated hydration

free energy using our model was -746.7 kcal/mol, compared to the -747.4 kcal/mol experimental result from Marcus (after corrections as described in the SI). To characterize the orientation of water molecules surrounding the ion, the radial distribution function (RDF) was calculated from MD simulation trajectory. From 10 ns MD simulation of a single La³⁺ ion in water using the new parameters, the RDF and coordination number of La³⁺····O have been derived (Figure 4). The RDF plot

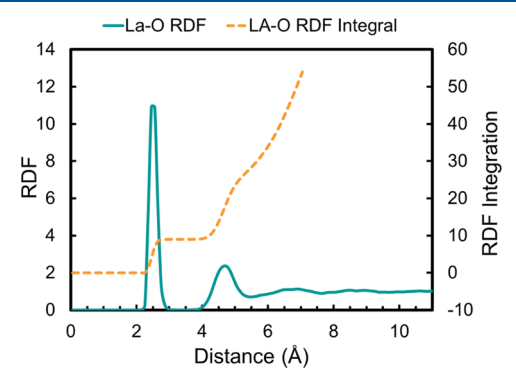


Figure 4. RDF and coordination number obtained from 2 ns AMOEBA molecular dynamics simulation of La^{3+} in water. Data are included in Table S4.

shows a sharp first peak located at 2.45-2.55 Å, indicating that water molecules in the first shell are tightly bound at that distance. The CN is ~9.0, which suggests that, on average, nine water molecules are found in the first shell. The second peak is at about 4.7 Å, and the CN indicates that there are about 16-17 water in the second shell. There is a vacuum gap of almost 1 Å between the first and second shells due to the aforementioned strong interaction between La^{3+} and the first-shell water molecules, similar to what was previously observed for multivalent cations with both ab initio molecular dynamics simulations and molecular dynamics simulations with AMOE-BA force fields. 17,59

For comparison, the CN of La³⁺ in aqueous solution is usually accepted as 8-9, and the PDB structure 7CCO shown in Figure 1B also demonstrates this same local solvation structure. 1,2,5,36 Marcus reported a mean ion—water internuclear distance of 2.53 Å in 1988^{60} and noted in 1991 that La^{3+} was coordinated by an average of 10.3 water molecules in its first hydration shell.⁵⁰ Näslund and co-authors reported large-angle X-ray scattering (LAXS) data for La^{3+} solvation in 1991, revealing a CN of 8–9, with first-shell interatomic distances of 2.52-2.66 Å and a second shell of ~18 water molecules at 4.63 Å. Allen et al. reported a CN of 9.2 with an actinide(O)...La³⁺ interatomic distance of 2.54 Å in 2000 but mentioned that statistical analysis of the synchrotron-based extended X-ray absorption finestructure (EXAFS) spectroscopy data could not differentiate definitively between a CN of 8 and 9.61 A theoretical study of La³⁺ using AMOEBA, conducted in 2005, found that La³⁺ was typically coordinated by nine water molecules in its first shell at ~2.56 Å and 16 water molecules in its second shell at a distance of \sim 4.68 Å.³¹ The increased first-shell distance in comparison to most of the experimental data shows that the 2005 La³⁺ AMOEBA model may have underestimated the strength of the water···La³⁺ interaction. Our new model has excellent agreement with the available experimental data.

As described in the Methods section, two sets of MD simulations were performed here to predict the water residence

time. In the 10 ns trajectory, up to about 5 ns of residence time can be observed. In the 1.2 ns simulation trajectory, the residence time shows a peak located at around 30 fs, which decays afterward (Figure 5). Our results indicate that, while

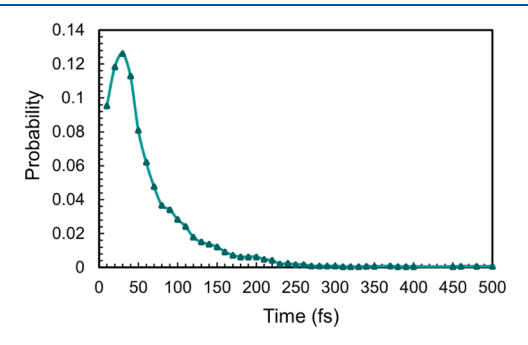


Figure 5. Distribution of the water residence time in the first solvation shell around La³⁺. Data are included in Table S5.

some water molecules stay several nanoseconds in the first hydration shell of La³⁺, most water molecules exchange quickly, and the most probable time scale is in the tens of fs. Our simulations were not long enough for us to infer the upper boundary on residence time.

La³⁺...Acetate Interaction. The interaction of the lanthanum cation with the acetate anion proved particularly challenging for the AMOEBA model. The predicted interaction energy was too repulsive at close contact distance compared to results from quantum mechanics calculations. To counter this limitation, our collaborators at the Ponder Lab at Washington University added the new POLPAIR function to the Tinker Molecular Mechanics software package to allow fine-tuning of polarization strength between specific ion pairs using pairwise damping parameters. Using this new functionality, we were able to match the distance-dependent interaction energy curve from QM calculations more closely, with an error of 0.2% in the equilibrium region and 2% (error within 10 kcal/mol) over the rest of the curve. Interaction energies were plotted for the La³⁺... CH₃COO⁻ bidentate interaction complexes at intermolecular distances ranging from 1.54 to 3.24 Å (Figure 6). The equilibrium distance was found to be 2.2 Å, with a QM interaction energy of -505.7 kcal/mol.

We were able to describe the bidentate La³⁺····CH₃COO⁻ complex well with both AMOEBA09 and AMOEBA22 force-field models; however, the monodentate interactions were overestimated. For the bidentate interaction, the AMOEBA22 result agreed with the QM result on the equilibrium distance of

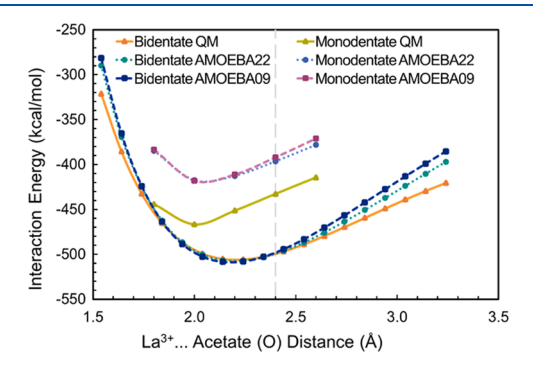


Figure 6. Interaction energies for the La³⁺···CH₃COO⁻ complex from QM and MM (AMOEBA09 and AMOEBA22) calculations.

2.2 Å, with AMOEBA09 showing a slightly shorter interaction distance. The QM interaction energies for these two distances (-505.04 and -505.66 kcal/mol) only differed by 0.6 kcal/mol, however. For both distances, AMOEBA09 and AMOEBA22 were within 1% of the QM interaction energies. In the case of the monodentate interactions, the interatomic distance at the minimum according to QM calculation (2.0 Å) was accurately described by AMOEBA09 and AMOEBA22, but the interaction energy differed by almost 50 kcal/mol. However, this value was still just over a 10% increase from QM (-466.7 kcal/mol).

There was a difficulty in optimizing a structure for monodentate La³⁺····CH₃COO⁻ to convergence as the CO bond stretched until it broke and oxygen became bound to La³⁺, even when starting from a reasonable monodentate La³⁺... CH₃COO⁻ complex conformation. To obtain a structure for the interaction energy calculations, a side chain involved in a monodentate interaction with La³⁺ in the PDB structure 7CCO was cut from the full structure, and hydrogens were added to form monodentate CH₃COO···La³⁺ (Figure S2). Alternatively, we could perform a geometry optimization while keeping the acetate frozen. Nonetheless, we decided to take the structure from an experimental PDB, as we believe it should be the most relevant orientation. The ion was then translated manually by ± 0.2 Å at a time to have complex structures with separations of 1.8-2.6 Å, and interaction energies at each distance were plotted (Figure 6). The dashed gray line in Figure 6 denotes the interatomic distance in 7CCO.

The difficulty in describing the monodentate binding conformation is similar to what we encountered in our previous studies of calcium and magnesium ions. In the case of the bidentate interactions, the two oxygen atoms can be described the same "atom type" due to resonance. For the monodentate interactions, the two oxygen atoms should be described differently, as the ion will stabilize the charge of and prefer to interact with one of the oxygens. If we were to model a static monodentate ion—acetate interaction structure, different parameters could be assigned to the oxygen that is binding with the ion, and we will be able to match QM energy very well. The challenge in MD simulations would be to handle the dynamics of ion—oxygen binding/unbinding, thus changing the state and parameters of oxygen atoms during the simulations.

La³⁺····Acetamide Interaction. Agreement between QM and our MM results for La³⁺····CH₃CONH₂ interaction energies are satisfactory, especially at shorter distances. The initial AMOEBA model was unable to replicate the shape of the distance-dependent interaction energy curve from QM accurately, leading to errors of up to 20 kcal/mol at distances beyond the equilibrium region. With the addition of POLPAIR, the interaction between lanthanum and acetamide was also modeled accurately-interaction energy and equilibrium distance were within 2 kcal/mol and 0.1 Å of the QM calculations. Interaction energies were plotted for complexes at intermolecular distances ranging from 1.49 to 3.09 Å (Figure 7). The interaction distance at the QM energetic minimum was 2.1 Å, with an energy of −186.7 kcal/mol. This distance was shifted slightly lower to 2.0 Å for AMOEBA09 and AMOEBA22. At this distance, the interaction energies were -186.4 kcal/mol for AMOEBA09 and -186.6 kcal/mol for AMOEBA22, with less than 1% change from the energy of -185.0 kcal/mol obtained using QM methods.

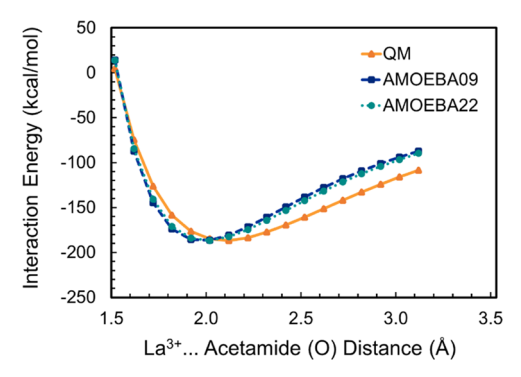


Figure 7. Interaction energies for the La³⁺····CH₃CONH₂ complex from QM and MM (AMOEBA09 and AMOEBA22) calculations.

CONCLUSIONS

We have developed two AMOEBA polarizable force-field models for simulation of La³⁺ with ligands responsible for the majority of La³⁺ interactions with biomolecules, such as lanmodulins. The main difference between the models based on AMOEBA09 and AMOEBA22 is that the latter includes improved, larger atomic polarizability for acetate and acetamide (Table S2). Interaction energies of La³⁺ with the representative molecules water, acetate, and acetamide have been carefully examined. The addition of a new scheme POLPAIR (pairwise damping) to Tinker provided the flexibility necessary for accurately capturing the strong and diverse polarization effects present in interactions between La3+ and both charged and neutral ligands, which was previously unfeasible. Using this new model, interaction energy calculations showed replication of QM energies and equilibrium interaction distances, as well as experimental hydration free energy of La³⁺. In general, the new AMOEBA model matches ab initio QM very well in equilibrium energy and distances, which will be crucial for accurate description of interactions in the binding pocket.

The calculated La³⁺···H₂O complex energy and coordination number (8-9) alone can explain most of the observed hydration free energy. From our simulations, nine water molecules were observed in the first solvation shell of La³⁺. The La³⁺-water interaction is much stronger than that of Ca^{2+} (-56.0 kcal/ mol),²² while the ion-O distances at minimum energy are similar at 2.2 Å (Ca²⁺) vs 2.3 Å (La³⁺). La³⁺ naturally attracts more water in the first solvation shell, some of which are tightly bound, while some exchange with the surroundings rapidly (within a few fs). Ion-acetate and ion-amide interactions are several times stronger than that of ion-water. Nonetheless, there will be significant energetic cost to overcome the repulsion between negatively charged acetate groups to assemble the binding pocket. The energetics and thermodynamics of La³⁺ binding to proteins will be evaluated in future work using an approach similar to that previously applied to Ca²⁺/Mg².²² The current model, including the newly added POLPAIR function, is now available for use in Tinker software, including the highperformance GPU implementation. The results of this work will enable classical molecular dynamics simulations of La³⁺ containing molecular systems including large protein complexes with much-needed accuracy and efficiency. Ultimately, these results, paired with such future studies, will enable a more comprehensive understanding of the complex ion-ligand interactions that will guide the development of potential bioinspired REM harvesting and separations.

ASSOCIATED CONTENT

Supporting Information

The Supporting Information is available free of charge at https://pubs.acs.org/doi/10.1021/acs.jpcb.2c07237.

Structures and parameters for complexes near the minima (TXT)

Details on basis sets used and interaction energy calculations as well as description of corrections to the experimental data used for comparison to our theoretical work; lanthanum containing PDB IDs; LigPlot+ figures showing La³⁺ interaction in the PDBs 6DAM, 6OC6, and 7CCO; structure of monodentate La³⁺ interaction with acetate; atomic polarizability parameters; interaction energies at minima predicted using QM, AMOEBA09, and AMOEBA22 models; and data used for calculating water RDF and water residence time (PDF)

AUTHOR INFORMATION

Corresponding Authors

Susan B. Rempe — Center for Integrated Nanotechnologies, Sandia National Laboratories, Albuquerque, New Mexico 87185, United States; orcid.org/0000-0003-1623-2108; Email: slrempe@sandia.gov

Pengyu Ren — Department of Biomedical Engineering, The University of Texas at Austin, Austin, Texas 78712, United States; ◎ orcid.org/0000-0002-5613-1910; Email: pren@mail.utexas.edu

Authors

Elizabeth E. Wait — Department of Biomedical Engineering, The University of Texas at Austin, Austin, Texas 78712, United States; Orcid.org/0000-0003-0953-2305

Justin Gourary — Department of Biomedical Engineering, The University of Texas at Austin, Austin, Texas 78712, United States

Chengwen Liu — Department of Biomedical Engineering, The University of Texas at Austin, Austin, Texas 78712, United States; Orcid.org/0000-0002-3930-7793

Erik D. Spoerke — Electronic, Optical, and Nano Materials Department, Sandia National Laboratories, Albuquerque, New Mexico 87185, United States; orcid.org/0000-0003-2286-2560

Complete contact information is available at: https://pubs.acs.org/10.1021/acs.jpcb.2c07237

Author Contributions

E.E.W. and J.G. were co-first authorship.

Note

The authors declare the following competing financial interest(s): Dr. Pengyu Ren is a co-founder of Qubit Pharmaceuticals.

ACKNOWLEDGMENTS

We acknowledge funding from the Laboratory Directed Research and Development Program and the University Partnerships Network Program at Sandia National Laboratories. This work was performed, in part, at the Center for Integrated Nanotechnologies, an Office of Science User Facility operated for the U.S. Department of Energy (DOE) Office of Science. Sandia National Laboratories is a multimission laboratory managed and operated by National Technology & Engineering Solutions of Sandia, LLC, a wholly owned subsidiary of

Honeywell International, Inc., for the U.S. DOE's National Nuclear Security Administration under contract DE-NA-0003525. This article has been authored by an employee of National Technology & Engineering Solutions of Sandia, LLC. The employee owns all right, title and interest in and to the article and is solely responsible for its contents. The United States Government retains and the publisher, by accepting the article for publication, acknowledges that the United States Government retains a non-exclusive, paid-up, irrevocable, world-wide license to publish or reproduce the published form of this article or allow others to do so, for United States Government purposes. The DOE will provide public access to these results of federally sponsored research in accordance with the DOE Public Access Plan https://www.energy.gov/downloads/doe-public-access-plan. The views expressed in the article do not necessarily represent the views of the U.S. DOE or the United States Government. PR is grateful for support by National Institutes of Health (R01GM114237) and Welch Foundation (F-2120).

REFERENCES

- (1) Cotruvo, J. A. The Chemistry of Lanthanides in Biology: Recent Discoveries, Emerging Principles, and Technological Applications. *ACS Cent. Sci.* **2019**, *5*, 1496–1506.
- (2) Deblonde, G. J. P.; Mattocks, J. A.; Park, D. M.; Reed, D. W.; Cotruvo, J. A.; Jiao, Y. Selective and Efficient Biomacromolecular Extraction of Rare-Earth Elements Using Lanmodulin. *Inorg. Chem.* **2020**, *59*, 11855–11867.
- (3) Park, D. M.; Brewer, A.; Reed, D. W.; Lammers, L. N.; Jiao, Y. Recovery of Rare Earth Elements from Low-Grade Feedstock Leachates Using Engineered Bacteria. *Environ. Sci. Technol.* **2017**, *51*, 13471–13480.
- (4) Pol, A.; Barends, T. R. M.; Dietl, A.; Khadem, A. F.; Eygensteyn, J.; Jetten, M. S. M.; Op den Camp, H. J. M. Rare Earth Metals Are Essential for Methanotrophic Life in Volcanic Mudpots: Rare Earth Metals Essential for Methanotrophic Life. *Environ. Microbiol.* **2014**, *16*, 255–264.
- (5) Cotruvo, J. A.; Featherston, E. R.; Mattocks, J. A.; Ho, J. V.; Laremore, T. N. Lanmodulin: A Highly Selective Lanthanide-Binding Protein from a Lanthanide-Utilizing Bacterium. *J. Am. Chem. Soc.* **2018**, 140, 15056–15061.
- (6) Wu, J. C.; Piquemal, J.-P.; Chaudret, R.; Reinhardt, P.; Ren, P. Polarizable Molecular Dynamics Simulation of Zn(II) in Water Using the AMOEBA Force Field. *J. Chem. Theory Comput.* **2010**, *6*, 2059–2070.
- (7) Jing, Z.; Liu, C.; Qi, R.; Ren, P. Many-Body Effect Determines the Selectivity for Ca2+ and Mg2+ in Proteins. *Proc. Natl. Acad. Sci. U.S.A.* **2018**, *115*, E7495–E7501.
- (8) Jing, Z.; Liu, C.; Cheng, S. Y.; Qi, R.; Walker, B. D.; Piquemal, J.-P.; Ren, P. Polarizable Force Fields for Biomolecular Simulations: Recent Advances and Applications. *Ann. Rev. Biophys.* **2019**, *48*, 371–394.
- (9) Jing, Z.; Liu, C.; Ren, P. Advanced Electrostatic Model for Monovalent Ions Based on Ab Initio Energy Decomposition. *J. Chem. Inf. Model.* **2021**, *61*, 2806–2817.
- (10) Jing, Z.; Rackers, J. A.; Pratt, L. R.; Liu, C.; Rempe, S. B.; Ren, P. Thermodynamics of Ion Binding and Occupancy in Potassium Channels. *Chem. Sci.* **2021**, *12*, 8920–8930.
- (11) Arabzadeh, H.; Liu, C.; Acevedo, O.; Ren, P.; Yang, W.; Albrecht-Schönzart, T. Hydration of Divalent Lanthanides, Sm²⁺ and Eu²⁺: A Molecular Dynamics Study with Polarizable AMOEBA Force Field. *J. Comput. Chem.* **2022**, *43*, 1286–1297.
- (12) Varma, S.; Rempe, S. B. Multibody Effects in Ion Binding and Selectivity. *Biophys. J.* **2010**, *99*, 3394–3401.
- (13) Gomez, D. T.; Pratt, L. R.; Asthagiri, D. N.; Rempe, S. B. Hydrated Anions: From Clusters to Bulk Solution with Quasi-Chemical Theory. *Acc. Chem. Res.* **2022**, *55*, 2201–2212.

- (14) Gomez, D. T.; Pratt, L. R.; Rogers, D. M.; Rempe, S. B. Free Energies of Hydrated Halide Anions: High Through-Put Computations on Clusters to Treat Rough Energy-Landscapes. *Molecules* **2021**, *26*, 3087.
- (15) Li, P.; Song, L. F.; Merz, K. M. Parameterization of Highly Charged Metal Ions Using the 12-6-4 LJ-Type Nonbonded Model in Explicit Water. *J. Phys. Chem. B* **2015**, *119*, 883–895.
- (16) Li, Z.; Song, L. F.; Li, P.; Merz, K. M. Parametrization of Trivalent and Tetravalent Metal Ions for the OPC3, OPC, TIP3P-FB, and TIP4P-FB Water Models. *J. Chem. Theory Comput.* **2021**, *17*, 2342–2354
- (17) Chaudhari, M. I.; Vanegas, J. M.; Pratt, L. R.; Muralidharan, A.; Rempe, S. B. Hydration Mimicry by Membrane Ion Channels. *Annu. Rev. Phys. Chem.* **2020**, *71*, 461–484.
- (18) Varma, S.; Rogers, D. M.; Pratt, L. R.; Rempe, S. B. Design Principles for K+ Selectivity in Membrane Transport. *J. Gen. Physiol.* **2011**, *137*, 479–488.
- (19) Rossi, M.; Tkatchenko, A.; Rempe, S. B.; Varma, S. Role of Methyl-Induced Polarization in Ion Binding. *Proc. Natl. Acad. Sci. U.S.A.* **2013**, *110*, 12978–12983.
- (20) Stevens, M. J.; Rempe, S. L. B. Ion-Specific Effects in Carboxylate Binding Sites. *J. Phys. Chem. B* **2016**, *120*, 12519–12530.
- (21) Stevens, M. J.; Rempe, S. L. B. Carboxylate Binding Prefers Two Cations to One. *Phys. Chem. Chem. Phys.* **2022**, 24, 22198–22205.
- (22) Jing, Z.; Qi, R.; Liu, C.; Ren, P. Study of Interactions between Metal Ions and Protein Model Compounds by Energy Decomposition Analyses and the AMOEBA Force Field. *J. Chem. Phys.* **2017**, *147*, No. 161733.
- (23) Xia, Z.; Wang, Q.; Mu, X.; Ren, P.Development of AMOEBA Force Field with Advanced Electrostatics. In *Molecular Modeling at the Atomic Scale: Methods and Applications in Quantitative Biology*; CRC Press, 2014; p 28.
- (24) Shi, Y.; Xia, Z.; Zhang, J.; Best, R.; Wu, C.; Ponder, J. W.; Ren, P. Polarizable Atomic Multipole-Based AMOEBA Force Field for Proteins. *J. Chem. Theory Comput.* **2013**, *9*, 4046–4063.
- (25) Liu, C.; Piquemal, J. P.; Ren, P. AMOEBA+ Classical Potential for Modeling Molecular Interactions. *J. Chem. Theory Comput.* **2019**, 15, 4122–4139.
- (26) Amezcua, M.; El Khoury, L.; Mobley, D. L. SAMPL7 Host—Guest Challenge Overview: assessing the reliability of polarizable and non-polarizable methods for binding free energy calculations. *J. Comput.-Aided Mol. Des.* **2021**, *35*, 1–35.
- (27) Jana, M.; MacKerell, A. D. CHARMM Drude Polarizable Force Field for Aldopentofuranoses and Methyl-Aldopentofuranosides. *J. Phys. Chem.* B **2015**, 119, 7846—7859.
- (28) Lemkul, J. A.; Huang, J.; Roux, B.; MacKerell, A. D. An Empirical Polarizable Force Field Based on the Classical Drude Oscillator Model: Development History and Recent Applications. *Chem. Rev.* **2016**, *116*, 4983–5013.
- (29) Lemkul, J. A.; MacKerell, A. D. Polarizable Force Field for DNA Based on the Classical Drude Oscillator: II. Microsecond Molecular Dynamics Simulations of Duplex DNA. J. Chem. Theory Comput. 2017, 13, 2072–2085.
- (30) Zhao, S.; Wei, H.; Cieplak, P.; Duan, Y.; Luo, R. *PyRESP*: A Program for Electrostatic Parameterizations of Additive and Induced Dipole Polarizable Force Fields. *J. Chem. Theory Comput.* **2022**, *18*, 3654–3670.
- (31) Clavaguéra, C.; Pollet, R.; Soudan, J. M.; Brenner, V.; Dognon, J. P. Molecular Dynamics Study of the Hydration of Lanthanum(III) and Europium(III) Including Many-Body Effects. *J. Phys. Chem. B* **2005**, 109, 7614–7616.
- (32) Vázquez-Montelongo, E. A.; Vázquez-Cervantes, J. E.; Cisneros, G. A. Current Status of AMOEBA—IL: A Multipolar/Polarizable Force Field for Ionic Liquids. *Int. J. Mol. Sci.* **2020**, *21*, 697.
- (33) Marjolin, A.; Gourlaouen, C.; Clavaguéra, C.; Ren, P. Y.; Wu, J. C.; Gresh, N.; Dognon, J. P.; Piquemal, J. P. Toward Accurate Solvation Dynamics of Lanthanides and Actinides in Water Using Polarizable Force Fields: From Gas-Phase Energetics to Hydration Free Energies. *Theor. Chem. Acc.* **2012**, *131*, No. 1198.

- (34) Marjolin, A.; Gourlaouen, C.; Clavaguéra, C.; Ren, P. Y.; Piquemal, J. P.; Dognon, J. P. Hydration Gibbs Free Energies of Open and Closed Shell Trivalent Lanthanide and Actinide Cations from Polarizable Molecular Dynamics. *J. Mol. Model.* **2014**, *20*, No. 2471.
- (35) Marjolin, A.; Gourlaouen, C.; Clavaguéra, C.; Dognon, J.-P.; Piquemal, J.-P. Towards Energy Decomposition Analysis for Open and Closed Shell F-Elements Mono Aqua Complexes. *Chem. Phys. Lett.* **2013**, *563*, 25–29.
- (36) Cook; Featherston; Showalter; Cotruvo. Structural Basis for Rare Earth Element Recognition by *Methylobacterium extorquens* Lanmodulin. *Biochemistry* **2019**, *58*, 120–125.
- (37) Burley, S. K.; Bhikadiya, C.; Bi, C.; Bittrich, S.; Chen, L.; Crichlow, G. V.; Christie, C. H.; Dalenberg, K.; Di Costanzo, L.; Duarte, J. M.; et al. RCSB Protein Data Bank: Powerful New Tools for Exploring 3D Structures of Biological Macromolecules for Basic and Applied Research and Education in Fundamental Biology, Biomedicine, Biotechnology, Bioengineering and Energy Sciences. *Nucleic Acids Res.* 2021, 49, D437–D451.
- (38) Ren, P.; Ponder, J. W. Polarizable Atomic Multipole Water Model for Molecular Mechanics Simulation. *J. Phys. Chem. B* **2003**, *107*, 5933–5947.
- (39) Ren, P.; Wu, C.; Ponder, J. W. Polarizable Atomic Multipole-Based Molecular Mechanics for Organic Molecules. *J. Chem. Theory Comput.* **2011**, *7*, 3143–3161.
- (40) Burnham, C. J.; Li, J.; Xantheas, S. S.; Leslie, M. The Parametrization of a Thole-Type All-Atom Polarizable Water Model from First Principles and Its Application to the Study of Water Clusters (n = 2-21) and the Phonon Spectrum of Ice Ih. *J. Chem. Phys.* **1999**, 110, 4566–4581.
- (41) Rackers, J. A.; Wang, Z.; Lu, C.; Laury, M. L.; Lagardère, L.; Schnieders, M. J.; Piquemal, J.-P. P.; Ren, P.; Ponder, J. W. Tinker 8: Software Tools for Molecular Design. *J. Chem. Theory Comput.* **2018**, 14, 5273–5289.
- (42) Gresh, N. Energetics of Zn2+ Binding to a Series of Biologically Relevant Ligands: A Molecular Mechanics Investigation Grounded On ab Initio Self-Consistent Field Supermolecular Computations. *J. Comput. Chem.* **1995**, *16*, 856–882.
- (43) Tiraboschi, G.; Gresh, N.; Giessner-Prettre, C.; Pedersen, L. G.; Deerfield, D. W. Parallel ab Initio and Molecular Mechanics Investigation of Polycoordinated Zn(II) Complexes with Model Hard and Soft Ligands: Variations of Binding Energy and of Its Components with Number and Charges of Ligands. *J. Comput. Chem.* 2000, 21, 1011–1039.
- (44) El Khoury, L.; Naseem-Khan, S.; Kwapien, K.; Hobaika, Z.; Maroun, R. G.; Piquemal, J.-P.; Gresh, N. Importance of Explicit Smeared Lone-Pairs in Anisotropic Polarizable Molecular Mechanics. Torture Track Angular Tests for Exchange-Repulsion and Charge Transfer Contributions: Importance of Explicit Smeared Lone-Pairs in Anisotropic Polarizable Molecular Mechanics. *J. Comput. Chem.* **2017**, 38, 1897—1920.
- (45) Neese, F.; Wennmohs, F.; Becker, U.; Riplinger, C. The ORCA Quantum Chemistry Program Package. J. Chem. Phys. 2020, 152, No. 224108
- (46) van Lenthe, E.; Snijders, J. G.; Baerends, E. J. The Zero-order Regular Approximation for Relativistic Effects: The Effect of Spin—Orbit Coupling in Closed Shell Molecules. *J. Chem. Phys.* **1996**, *105*, No. 13.
- (47) Guo, Y.; Riplinger, C.; Becker, U.; Liakos, D. G.; Minenkov, Y.; Cavallo, L.; Neese, F. Communication: An Improved Linear Scaling Perturbative Triples Correction for the Domain Based Local Pair-Natural Orbital Based Singles and Doubles Coupled Cluster Method [DLPNO-CCSD(T)]. *J. Chem. Phys.* **2018**, *148*, No. 011101.
- (48) Hong, G.; Dolg, M.; Li, L. A Comparison of Scalar-Relativistic ZORA and DKH Density Functional Schemes: Monohydrides, Monooxides and Monofluorides of La, Lu, Ac and Lr. *Chem. Phys. Lett.* **2001**, 334, 396–402.
- (49) Wang, L.-P.; Martinez, T. J.; Pande, V. S. Building Force Fields: An Automatic, Systematic, and Reproducible Approach. *J. Phys. Chem. Lett.* **2014**, *5*, 1885–1891.

- (50) Marcus, Y. Thermodynamics of Solvation of Ions. Part 5.—Gibbs Free Energy of Hydration at 298.15 K. *J. Chem. Soc., Faraday Trans.* **1991**, 87, 2995–2999.
- (51) Grossfield, A.; Ren, P.; Ponder, J. W. Ion Solvation Thermodynamics from Simulation with a Polarizable Force Field. *J. Am. Chem. Soc.* **2003**, *125*, 15671–15682.
- (52) Bussi, G.; Donadio, D.; Parrinello, M. Canonical Sampling through Velocity Rescaling. *J. Chem. Phys.* **2007**, *126*, No. 014101.
- (53) Wang, Z.Tinker9: Next Generation of Tinker with GPU Support, 2021. https://github.com/TinkerTools/tinker9.
- (54) Romo, T. D.; Leioatts, N.; Grossfield, A.Lightweight Object Oriented Structure Analysis: Tools for building tools to analyze molecular dynamics simulations, *J. Comput. Chem.*, 2014, 35, 2305—2318. https://github.com/GrossfieldLab/loos. DOI: 10.1002/jcc.23753.
- (55) Laskowski, R. A.; Swindells, M. B. LigPlot+: Multiple Ligand-Protein Interaction Diagrams for Drug Discovery. *J. Chem. Inf. Model.* **2011**, *51*, 2778–2786.
- (56) Litman, J. M.; Liu, C.; Ren, P. Atomic Polarizabilities for Interactive Dipole Induction Models. *J. Chem. Inf. Model.* **2022**, 62, 79–87.
- (57) The PyMOL Molecular Graphics System, Version 1.8; Schrödinger, LLC2015.
- (58) Pratt, L. R.; Rempe, S. B.Quasi-Chemical Theory and Implicit Solvent Models for Simulations. In *Simulation and Theory of Electrostatic Interactions in Solution*; ASCE: Sante Fe, New Mexico (USA), 1999; pp 172–201.
- (59) Zhang, J.; Yang, W.; Piquemal, J. P.; Ren, P. Modeling Structural Coordination and Ligand Binding in Zinc Proteins with a Polarizable Potential. *J. Chem. Theory Comput.* **2012**, *8*, 1314–1324.
- (60) Marcus, Y. Ionic Radii in Aqueous Solutions. Chem. Rev. 1988, 88, 1475-1498.
- (61) Allen, P. G.; Bucher, J. J.; Shuh, D. K.; Edelstein, N. M.; Craig, I. Coordination Chemistry of Trivalent Lanthanide and Actinide Ions in Dilute and Concentrated Chloride Solutions. *Inorg. Chem.* **2000**, 39, 595–601.

